

Monte Carlo simulations of corrosion inhibition of mild steel in 0.5 M sulphuric acid by some green corrosion inhibitors

K. F. Khaled

Received: 30 January 2009 / Revised: 30 March 2009 / Accepted: 6 April 2009 / Published online: 9 May 2009
© Springer-Verlag 2009

Abstract Atomistic modelling and simulations are becoming increasingly important in the field of corrosion inhibition. New research and development efforts and new possibilities for using computational chemistry in studying the behaviour of corrosion inhibitors on the metal surfaces are introduced. In this study, Monte Carlo simulations technique incorporating molecular mechanics and molecular dynamics were used to simulate the adsorption of methionine derivatives, namely L-methionine, L-methionine sulphoxide and L-methionine sulphone, on iron (110) surface in 0.5 M sulphuric acid. Adsorption energy as well as hydrogen bond length has been calculated. Results show that methionine derivatives have a very good inhibitive effect for corrosion of mild steel in 0.5 M sulphuric acid solution. Tafel polarisation studies have shown that methionine derivatives act as mixed-type inhibitors, and their inhibition mechanism is adsorption assisted by hydrogen bond formation. Impedance results indicate that the values of the constant phase element tend to decrease with increasing methionine derivatives concentrations due to the increase in the thickness of the electrical double layer. In addition, both polarisation resistance and inhibition efficiency $E_i(\%)$ tend to increase with increasing inhibitors concentrations due to the increase of the surface coverage, i.e., the decrease of the

electrochemical active surface area. The quantum mechanical approach may well be able to foretell molecular structures that are better for corrosion inhibition.

Keywords Monte Carlo simulations · Corrosion inhibition · Green corrosion inhibitors · EIS · Quantum chemical calculation

Introduction

Corrosion of iron and steels is a major concern in the petrochemical industry due to the destructive attack of iron substrates by chemical and electrochemical reactions. One common approach to control such corrosion is to add small amounts of organic compounds (inhibitors) to the production fluid. Owing to increasing ecological awareness and strict environmental regulations and the need to develop environmentally friendly processes, attention is now focused on the development of substitute nontoxic alternatives to inorganic inhibitors applied earlier. Natural products extracted from plant sources [1–5], as well as some non toxic organic compounds, which contain polar functions with nitrogen, oxygen and/or sulphur in conjugated systems in their molecules [5–12], have been effectively used as inhibitors in many corrosion systems. Amino acids are attractive as corrosion inhibitors because they are relatively easy to produce with high purity at low cost and are soluble in aqueous media. Certain amino acids have been tested as inhibitors of Ni [13], Co [14], and mild steel [15] corrosion in H_2SO_4 [13–17].

Methionine derivatives are sulphur-containing amino acids. Methionine itself is investigated as possible corrosion inhibitor for mild steel [5, 18–22] and of low carbon steel [23]. Ashassi-Sorkhabi et al. [24] reported the successful

K. F. Khaled (✉)
Electrochemistry Research Laboratory, Chemistry Department,
Faculty of Education, Ain Shams University, Roxy,
Cairo 11711, Egypt
e-mail: khaledrice2003@yahoo.com

K. F. Khaled
Materials and Corrosion Laboratory, Chemistry Department,
Faculty of Science, Taif University,
Taif, Kingdom of Saudi Arabia

application of methionine as a corrosion inhibitor for aluminium in mixed acid solution and pointed out the role of S atom in increasing the interaction of the molecule with the metal surface. Morad et al. [5], in their study of the inhibiting effect of methionine on mild steel corrosion in phosphoric acid, observed that the adsorption of methionine onto the metal surface obeyed the Frumkin isotherm with an adsorption free energy ($\Delta G_{\text{ads}}^{\circ}$) value of 25.4 kJ mol^{-1} . Abd-El-Nabey et al. [19] showed that methionine adsorbed on mild steel surface in 0.5 M sulphuric acid in two steps: A monolayer of the adsorbate is formed on the metal surface, and this is followed by the deposition of a second adsorbate layer.

The interactions between metal substrate and inhibitors are not very well understood. Therefore, a molecular level understanding of metal–inhibitor interactions on iron is much desirable, which could provide insights into the design of inhibitor systems with superior properties.

For the last decades, quantum chemistry has become an effective way to study the correlation of the molecular structure and its inhibition properties, and much achievement was reached; human's knowledge of mechanism of corrosion inhibition penetrates to the microscopic level [25–29]. From the 1970s, Vosta researched the relationship between the quantum chemical parameters and inhibition efficiency using Huckel molecular orbital theory [30]; Costa explained the mechanism of corrosion inhibition of different linear chain diols, diamines and aliphatic amino alcohols using the semi-empirical MINDO/3-SCF method [31]; Jingchang Zhang calculated the structure of N-contained compounds using HOMO method, discovering that the electronic density and highest occupied molecular orbital (HOMO) energy level of active group is in relation to inhibition efficiency [32]; Abdul Ahad calculated a series of p-substituted aniline using semi-empirical CNDO/2 method and obtained significant correlations between corrosion rate and corrosion current with the chemical indices of the inhibitors [33]; Daxi Wang calculated the molecular geometry and chemical adsorption of six imidazolines and Fe atom by MNDO and CNDO/2M methods and discussed their inhibition performance [34, 35]. However, quantum chemistry computing methods, such as ab initio and semi-empirical methods, are computationally expensive and are usually only applied to systems containing no more than 100 atoms or small molecules. It is not practical to model large systems containing dozens of metal atoms and hundreds of solvent molecules. The molecular dynamics (MD) method is often used to study the interaction of phase interfaces [36, 37], only a few works have been done to research the interaction of inhibitors with the metal surface [38, 39].

To be able to reveal new and effective corrosion inhibitors, the interactions between the inhibitor molecules

and the metal surfaces should by all means be explained and understood in details. In examining these interactions, theoretical approaches can be applied very usefully. Therefore, recently, a trend and an increasing attention were seen on the involvement of these theoretical approaches in corrosion studies [40–55].

The aim of the present work is to study the influence of some selected sulphur-containing amino acids, namely L-methionine (MIT), L-methionine sulphoxide (MITO) and L-methionine sulfone (MITO2), on the inhibition of mild steel corrosion in 0.5 M H_2SO_4 solutions using chemical (weight loss), electrochemical techniques (potentiodynamic polarisation and electrochemical impedance spectroscopy) as well as explicit solvent simulations using molecular dynamics and quantum chemical calculation to explore the adsorption mechanism of these amino acids on iron surface (110). In addition, as the electronic structure of these amino acids could be involved in determining interaction with iron surface, therefore, correlation between certain molecular orbital calculations and inhibitor efficiencies will be sought.

Experimental procedures

Computational details

Understanding adsorption phenomena is of key importance in corrosion problems. Monte Carlo simulations help in finding the most stable adsorption sites on metal surfaces through finding the low-energy adsorption sites on both periodic and nonperiodic substrates or to investigate the preferential adsorption of mixtures of adsorbate components. Materials studio 4.3, software from Accelrys, Inc. [56] has been used to build methionine derivatives, iron surface and solvent molecules. In addition, the periodic structures can be built using the tools available in the Materials studio for building crystals and surfaces. Molecular mechanics tools are used to investigate the corrosion system. The key approximation in these studies that the potential energy surface, on which the atomic nuclei move, is represented by a classical force field, which are developed by parameterising data from experiment and high level quantum mechanical calculations. COMPASS stands for condensed-phase optimised molecular potentials for atomistic simulation studies [57], which is used to optimise the structures of all components of the system of interest (iron substrate/solvent/inhibitor). It is the first ab initio force field that enables accurate and simultaneous prediction of chemical properties (structural, conformational, vibrational, etc.) and condensed-phase properties (equation of state, cohesive energies, etc.) for a broad range of chemical systems. It is also the first high-quality force

field to consolidate parameters of organic and inorganic materials.

The first step in this computational study is the preparation of a model of molecules, which will adsorb on the surface with optimised geometry (i.e. energy minimised). Among the different steps involved in the modelling approach is the construction of the iron surface from the pure crystal, the addition of the methionine derivatives near to the surface, the definition of the potentials (i.e. the force field) to study the liquid–solid interaction, followed by the geometry optimization calculation. This particular case, the use of molecular mechanics can be seen as a precursor to computationally more expensive quantum mechanical methods: Once the model has been optimised with suitable force field (COMPASS), we will be able to simulate a substrate (iron surface) loaded with an adsorbate (methionine derivatives), taking into consideration the solvent effect. This computational study aims to find low-energy adsorption sites to investigate the preferential adsorption of methionine derivatives on iron surface aiming to find a relation between the effect of their molecular structure and their inhibition efficiency.

To build iron surface, amorphous cell module has been used to create solvent/methionine derivative cell on iron surface. The behaviour of the three selected methionine derivatives on the surface was studied using molecular dynamics simulations and the COMPASS force field. The MD simulation of the interaction between the methionine derivatives dissolved in H₂O and the iron surface (110) was carried out in a simulation box (2.3×2.3×1.9 nm) with periodic boundary conditions in order to simulate a representative part of an interface devoid of any arbitrary boundary effects. A cutoff distance of 1.0 nm with a spline switching function was applied for the non-bond interactions, i.e. for coulombic, van der Waals and hydrogen bond interactions. The cutoff used to select the spline width, which specifies the size of the region within which non-bond interactions, are splined from their full value to zero. For the actual computation of this interaction, energy charge groups are used. Cutoff distance specifies the distance at which to exclude interactions from the non-bond list. The iron crystal is cleaved along with the (110) plane, thus representing the iron surface. For the MD simulation, all the spatial positions of the iron atoms in the simulation box are fixed because the thermal vibrations of the interaction with an adsorbed molecule and not in the physical behaviour of the crystal itself. The liquid phase consists of 350 H₂O molecules and a single dissolved inhibitor molecule. On top of this “aqueous layer”, an additional layer of 150 H₂O molecules with fixed spatial positions serves as an upper limit for the liquid phase acting like a wall but with the same physical and chemical properties. The MD simulation simulates a substrate loaded

with an adsorbate. A low-energy adsorption site is identified by carrying out a Monte Carlo search of the configurational space of the substrate–adsorbate system as the temperature is slowly decreased. This process is repeated to identify further local energy minima. During the course of the simulation, adsorbate molecule are randomly rotated and translated around the substrate. The configuration that results from one of these steps is accepted or rejected according to the selection rules of the Metropolis Monte Carlo method [58]. The force field used is COMPASS, charge is force field assigned, quality is fine and summation method is group- and atom based. All structures used in this study are minimised in order to ensure that the energy results used in calculating the adsorption energy are accurate; it is critically important that when we optimise the structures, we use the same energy minimization settings as we intend to use for calculating the adsorption energy of methionine derivatives. This includes not only the force field, atomic charges, and non-bond summation methods but also the quality of the energy and geometry optimization calculations and the convergence tolerances used for the minimization.

Quantum chemical calculations carried out using Dewar’s linear combinations of atomic orbitals–self-consistent field–molecular orbital (LCAO–SCF–MO) [59]. We used PM3 semi-empirical method in commercially available quantum chemical software Hyperchem, release 8.06 [60]. A full optimization of all geometrical variables without any symmetry constraint was performed at the restricted Hartree–Fock level. It develops the molecular orbitals on a valence basis set and also calculates electronic properties and the optimised geometries of the methionine derivatives molecules. As an optimization procedure, the built-in Polak–Ribiere algorithm was used [61].

Inhibitors

All studied compounds included, such as MIT, MITO and MITO2, are bought from Sigma-Aldrich Chemical and were used without further purification. All compounds were used without pretreatment in the concentration range of 5×10^{-2} to 10^{-4} M. The electrodes were immersed in 0.5 M H₂SO₄ (Fisher Scientific) for 60 min before starting measurements. All experiments were conducted at $25 \pm 1^\circ\text{C}$. The electrolyte solution was made from analytical reagent grad, H₂SO₄.

Chemical and electrochemical measurements

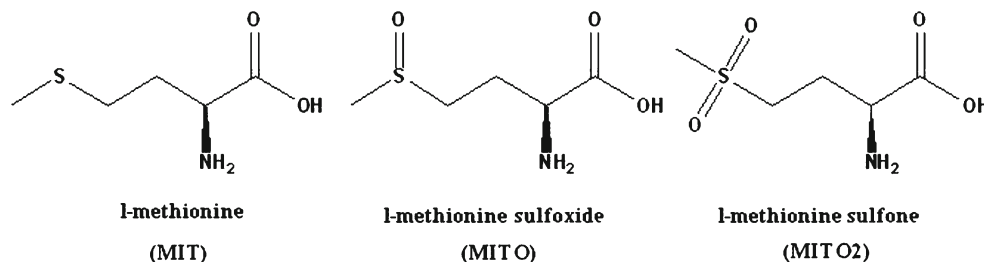
Gravimetric experiments were carried out in a double glass cell equipped with a thermostated cooling condenser. The solution volume was 100 ml. The iron specimens used have a rectangular form (length=2 cm, width=1 cm and

thickness=0.06 cm). The duration of tests was 6 h at $25 \pm 1^\circ\text{C}$. Duplicate experiments were performed in each case, and the mean value of the weight loss is reported. Weight loss allowed calculation of the mean corrosion rate in ($\text{g cm}^{-2} \text{h}^{-1}$).

Electrochemical experiments were carried out using a conventional electrolytic cell [62] with three-electrode arrangement: saturated calomel reference electrode (SCE), platinum wire (Premion[®] 99.99%) and 99.9% Pt gauze (52 mesh, Johnson Matthey) as a counter-electrode and a mild steel rod working electrode (C=0.12%, Mn=0.85%, S=

0.055%, P=0.05%, Si=0.09% and the remainder iron). All reported potentials are given versus the SCE.

A mild steel rod with surface area of 0.5 cm^2 , mounted in Teflon, was abraded using emery papers of 180, 120, 2/0 and 4/0 grit in order. It was polished with Al_2O_3 ($0.5 \mu\text{m}$ particle size), cleaned in $18 \text{ M}\Omega$ water in an ultrasonic bath and rinsed with acetone and bi-distilled water; the same procedure was used in case of gravimetric experiments. Chemical structures of the studied compounds are presented below.



The electrodes were arranged in such a way that one-dimensional potential field existed over the WE surface in solution. To get an impression about the process occurred at the iron/acid interface, Tafel curves were obtained by changing the electrode potential automatically from (-250 to $+250 \text{ mV}_{\text{SCE}}$) versus open circuit potential with scan rate of 1 mV/s . In addition, electrochemical impedance spectroscopy (EIS) measurements were carried out in a frequency range of 100 kHz – 30 mHz with amplitude of 10 mV peak-to-peak using ac signals at open circuit potential.

Measurements were performed using Gamry Instrument Potentiostat/Galvanostat/ZRA. This includes a Gamry Framework system based on the ESA400, Gamry applications that include DC105 for dc corrosion measurements, EIS300 for electrochemical impedance spectroscopy measurements along with a computer for collecting data. Echem Analyst 4.0 software was used for plotting, graphing and fitting data.

Results and discussions

Computational study

Before performing Monte Carlo simulation, molecular dynamics techniques are applied on a system comprising a methionine derivatives, solvent molecules and iron surface. Methionine derivatives is placed on the surface, optimise and then run quench molecular dynamics. Figure 1 shows the optimization energy curves for the three studied

molecules before putting them on the iron surface. It can be seen from Fig. 1 that MITO2 has the lowest optimization energy, which suggests the stability of this molecule compared with the other methionine derivatives. Total energy, average total energy, van der Waals energy, electrostatic energy and intramolecular energy for methionine/solvent/iron surface are calculated by optimising the whole system and presented in Fig. 2.

The Monte Carlo simulation process tries to find the lowest energy for the whole system. The structures of the adsorbate components (methionine derivatives) are minimised until they satisfy certain specified criteria. The Metropolis Monte Carlo method used in this simulation, samples the configurations in an ensemble by generating a

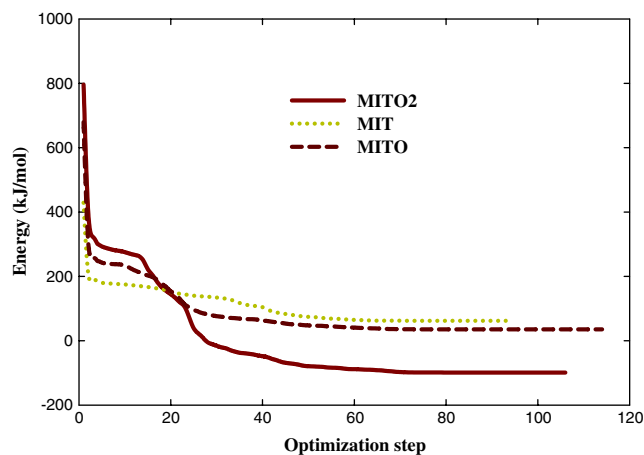


Fig. 1 Optimization energy curves for the studied molecules before putting them on the iron surface

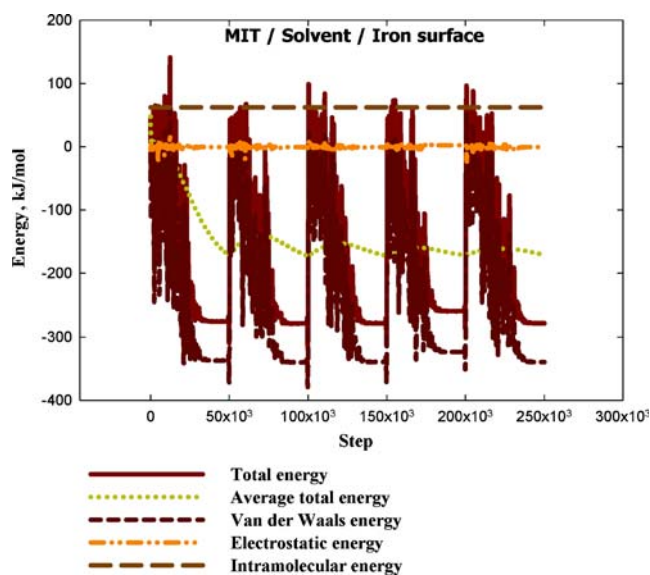


Fig. 2 Total energy distribution for methionine/solvent/iron system

chain of configurations, for example m, n, \dots . The step that transforms configuration m to n is a two-stage process. First, a trial configuration is generated with probability α_{mn} . Then, either the proposed configuration, n , is accepted with a probability P_{mn} or the original configuration, m , is retained with a probability $1 - P_{mn}$. The overall transition probability, π_{mn} , is thus obtained from Eq. 1:

$$\pi_{mn} = \alpha_{mn} P_{mn} \quad (1)$$

This geometry optimization is carried out using an iterative process, in which the atomic coordinates are adjusted until the total energy of a structure is minimised, i.e. it corresponds to a local minimum in the potential energy surface. The geometry optimization process is based on reducing the magnitude of calculated forces until they become smaller than defined convergence tolerances. The forces on an atom are calculated from the potential energy expression and will, therefore, depend on the force field that is selected (COMPASS). The outputs and descriptors calculated by the Monte Carlo simulation are presented in Table 1. The parameters presented in Table 1 include total energy, in kJ mol^{-1} , of the substrate–adsorbate configuration. The total energy is defined as the sum of the energies of the adsorbate components, the rigid adsorption energy

and the deformation energy. In this study, the substrate energy (iron surface) is taken as zero. In addition, adsorption energy in kJ mol^{-1} , reports energy released (or required) when the relaxed adsorbate components (methionine derivatives) are adsorbed on the substrate. The adsorption energy is defined as the sum of the rigid adsorption energy and the deformation energy for the adsorbate components. The rigid adsorption energy reports the energy, in kJ mol^{-1} , released (or required) when the unrelaxed adsorbate components (i.e., before the geometry optimization step) are adsorbed on the substrate. The deformation energy reports the energy, in kJ mol^{-1} , released when the adsorbed adsorbate components are relaxed on the substrate surface. Table 1 shows also (dE_{ads}/dN_i) , which reports the energy, in kJ mol^{-1} , of substrate–adsorbate configurations where one of the adsorbate components has been removed.

As can be seen from Table 1, MITO2 gives the maximum adsorption energy in negative value found during the simulation process. High values of adsorption energy indicate that MITO2 molecule will give the highest inhibition efficiency. The close contacts between methionine derivatives and iron surface, the best adsorption configuration for the studied compounds as well as the possibility of hydrogen bond formation are shown in Fig. 3. From the molecular structure of iron, it is evident that the unoccupied d-orbital exhibits a tendency to obtain electron. Methionine and its derivative, which are discussed in the present work, has a number of lone-pair electrons containing atoms like N, O and sulphur, making it possible to provide electrons to the unoccupied orbitals of iron, to form a stable coordination bond. Therefore, the studied molecules are likely to adsorb on the iron surface to form stable ad layers and protect iron from corrosion. The following parameters derived from the quantum chemical calculations are considered.

Quantum chemical calculations

Methionine derivatives are molecules containing the amino functional group ($-\text{NH}_2$), carboxylic group ($-\text{COOH}$) attached to sulphur, sulfoxide and sulfone groups in MIT, MITO and MITO2, respectively. The reactive ability of the methionine derivatives are considered to be closely related to their frontier molecular orbitals, the HOMO and LUMO.

Table 1 Outputs and descriptors calculated by the Monte Carlo simulation for adsorption of methionine derivatives on iron (110)

Inhibitor	Total energy (kJmol^{-1})	Adsorption energy (kJmol^{-1})	Rigid adsorption energy (kJmol^{-1})	Deformation energy (kJmol^{-1})	dE_{ads}/dN_i (kJmol^{-1})	Calculated hydrogen bond/nm
MITO2	-310.86	-234.15	-227.26	-6.88	-234.15	0.21
MITO	-321.15	-156.13	-160.98	4.85	-156.13	0.25
MIT	-290.09	-132.35	-138.15	5.79	-132.35	0.28

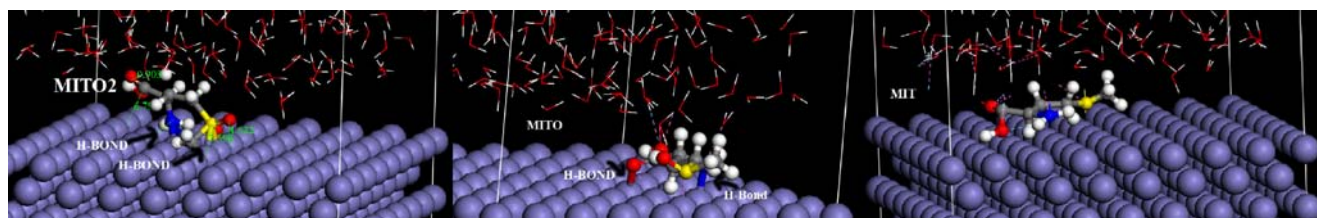


Fig. 3 Mode of adsorption of the methionine derivatives on iron (110)

Higher HOMO energy (E_{HOMO}) of the molecule means a higher electron donating ability to appropriate acceptor molecules with low-energy empty molecular orbital. Figure 4 shows structure of methionine derivatives, molecular orbital plots and the charge density distribution. It is worth noting that the charge density distribution on MITO2 is more intense than MITO and MIT, which enhance the possibility of MITO2 to adsorb more strongly on iron surface than MITO and MIT. It is confirmed that the more negative the atomic charges of the adsorbed centre, the more easily the atom donates its electrons to the unoccupied orbital of metal [63]. Therefore, these negative atomic charges indicated that nitrogen, sulphur and oxygen atoms are the possible active adsorption sites.

A hard molecule has a large energy gap, and a soft molecule has a small energy gap. Soft molecules are more

reactive than hard molecules, in general. Moreover, the gap between the HOMO and LUMO energy levels of the molecules is another important factor that should be considered. Excellent corrosion inhibitors are usually those organic compounds that not only offer electrons to unoccupied orbital of the metal surface but also accept free electrons from the metal [4, 64]. The energy gap between HOMO and LUMO indicates that the smaller energy gap results in a high corrosion inhibition implying soft–soft interaction. It is well established in the literature that the higher the HOMO energy of the inhibitor, the greater the trend of offering electrons to unoccupied d orbital of the metal, and the higher the corrosion inhibition efficiency. In addition, the lower the LUMO energy, the easier the acceptance of electrons from metal surface, as the LUMO–HOMO energy gap decreased and the efficiency of inhibitor

Fig. 4 Structure of methionine derivatives, molecular orbital plots, and the charge density distribution

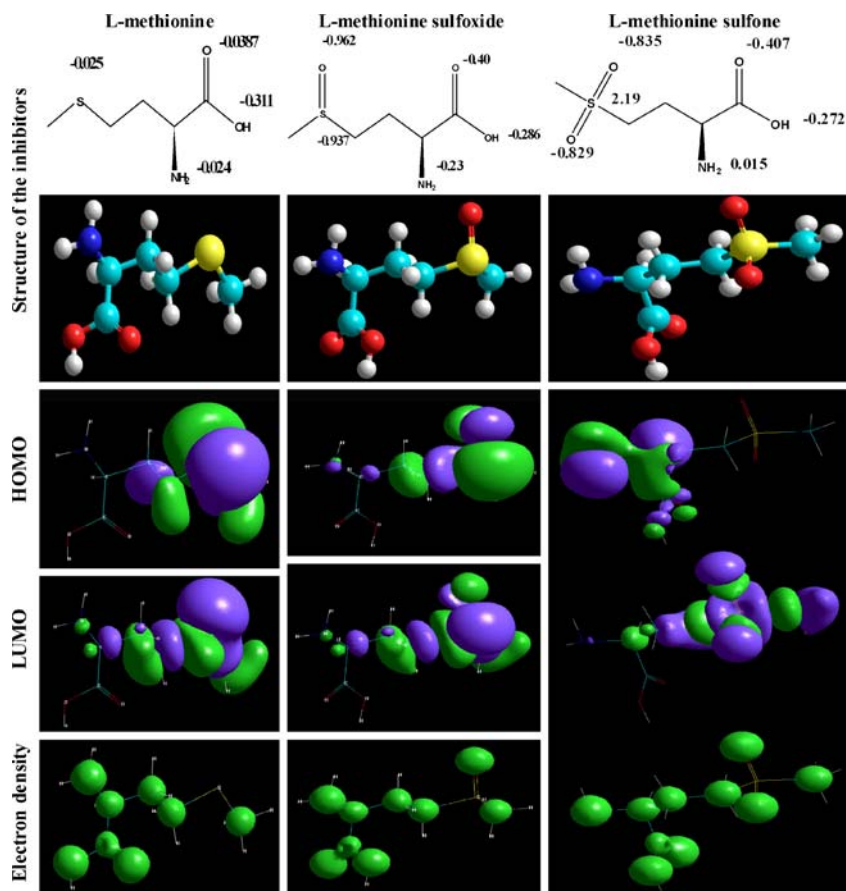


Table 2 Theoretical quantum chemical calculations using semi-empirical SCF-MO method (PM3) in Hyperchem 8.06 programme for methionine derivatives

Inhibitor	E_{HOMO} (kJ)	E_{LUMO} (kJ)	$\Delta = E_{LUMO} - E_{HOMO}$ (kJ)	μ (D)
MITO2	-866.52	24.04	890.63	1.131
MITO	-918.85	-1.48	917.41	2.42
MIT	-969.73	-18.53	951.20	3.82

improved. Quantum chemical parameters listed in Table 2 reveal that (MITO2) has the highest HOMO and the lowest LUMO. In addition, Table 2 shows that, for high inhibition efficiency, the dipole moment (μ) of the inhibitor molecules should be low. The experimental measurements are used to investigate this computational approach. The inhibition of the methionine derivatives was determined experimentally by using weight loss and electrochemical techniques.

Weight loss measurements

The corrosion of mild steel in 0.5 M H_2SO_4 in the absence and presence of MIT, MITO and MITO2 was investigated at $25 \pm 1^\circ C$ using weight loss measurements. The calculated values of corrosion rate (in $g\ cm^{-2}\ h^{-1}$), inhibition efficiency $E_w(\%)$ and surface coverage (θ) for iron corrosion in 0.5 M H_2SO_4 (blank) and in the presence of different concentrations of inhibitors (MIT, MITO and MITO2) from the weight loss measurement are shown in Table 3. Data in Table 3 indicate that corrosion rate depends on the nature and concentration of the compounds under investigation. The inhibition efficiency $E_w(\%)$ and surface coverage (θ) were evaluated using the following equations:

$$\text{Inhibition efficiency } E_w(\%) = \left(1 - \frac{w}{w_o}\right) \times 100 \quad (2)$$

$$\text{Surface coverage } (\theta) = \left(1 - \frac{w}{w_o}\right) \quad (3)$$

where w and w_o are the weight losses of iron in inhibited and uninhibited solutions, respectively.

The difference between the inhibitors is best seen in the middle concentration range, reflecting the influence of the molecular structure on their protective properties. Based on the maximum inhibitor efficiency, the methionine derivatives are ranked as follows:

MITO2 > MITO > MIT.

The gravimetric investigations show that all compounds exhibit inhibition properties, the best being the MITO2. Thus, weight loss measurements, in accordance with Monte Carlo simulations, demonstrate that all the studied methi-

online derivatives exhibit inhibition properties, and the most effective one is MITO2 derivative.

Tafel polarisation measurements

Polarisation curves of the mild steel electrode in 0.5 M H_2SO_4 with and without the addition of MITO2, MITO and MIT at different concentrations are shown in Figs. 4, 5 and 6. As can be seen, both cathodic and anodic reactions of mild steel electrode corrosion were inhibited with the increase of methionine derivatives concentrations in 0.5 M H_2SO_4 . Methionine derivatives suppressed both cathodic and anodic reactions. This result suggests that the addition of methionine derivatives reduces anodic dissolution of mild steel and also retards the hydrogen evolution reaction. Tafel lines of nearly equal slopes were obtained, indicating that the hydrogen evolution reaction was under activation control. The constancy of the cathodic slope may have indicated that the mechanism of proton discharge reaction did not change by the addition of methionine derivatives (Fig. 7).

Table 4 represents the values of the associated electrochemical parameters such as corrosion potential E_{corr} , cathodic and anodic Tafel slopes (β_c and β_a), corrosion current density i_{corr} obtained by extrapolation of the Tafel lines and the calculated inhibition efficiencies $E_p(\%)$ are reported from the following equation:

$$\text{Inhibition efficiency } E_p = \left(1 - \frac{i_{corr}}{i_{corr}^o}\right) \times 100 \quad (4)$$

where i_{corr} and i_{corr}^o are inhibited and uninhibited corrosion current densities, respectively.

Table 3 Corrosion rate in ($g\ cm^{-2}\ h^{-1}$), inhibition efficiency data obtained from weight loss measurements in iron in absence of various concentrations of methionine derivatives in 0.5 M H_2SO_4 at $25 \pm 1^\circ C$

	Conc. M	Corrosion rate ($g\ cm^{-2}\ h^{-1}$)	Surface coverage (θ)	$E_w(\%)$
	Blank	4.98×10^{-3}		
MIT	10^{-4}	1.14×10^{-3}	0.77	77.18
	10^{-3}	5.87×10^{-4}	0.88	88.21
	5×10^{-3}	4.43×10^{-4}	0.91	91.11
	5×10^{-2}	3.38×10^{-4}	0.93	93.21
MITO	10^{-4}	8.12×10^{-4}	0.83	83.69
	10^{-3}	4.88×10^{-4}	0.90	90.20
	5×10^{-3}	3.735×10^{-4}	0.92	92.50
	5×10^{-2}	2.988×10^{-4}	0.94	94.00
MITO2	10^{-4}	4.233×10^{-4}	0.91	91.50
	10^{-3}	3.327×10^{-4}	0.93	93.32
	5×10^{-3}	2.2×10^{-4}	0.95	95.58
	5×10^{-2}	8.96×10^{-5}	0.98	98.20

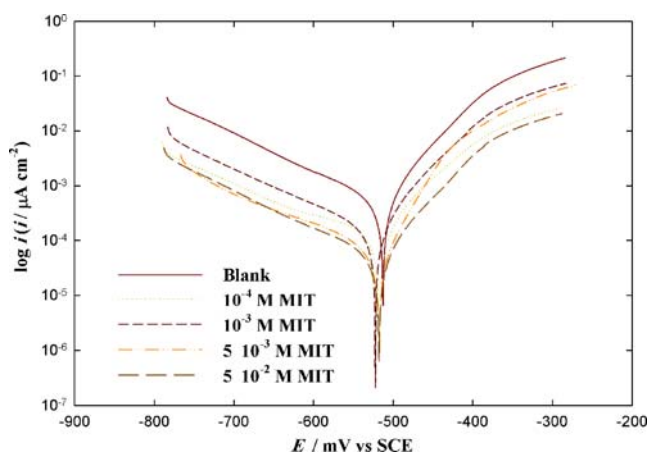


Fig. 5 Anodic and cathodic Tafel polarisation curves for mild steel in 0.5 M H₂SO₄ in the absence and presence of various concentrations of MIT at 25±1°C

As it can be seen from these polarisation results, the i_{corr} values decreased considerably in the presence of methionine derivatives and decreased with increasing inhibitor concentration. The addition of methionine derivatives modifies slightly the values of β_c . Both anodic and cathodic reactions are affected by the methionine derivatives. Based on these results, methionine derivatives are considered as mixed-type inhibitors. This means that the addition of methionine derivatives to 0.5 M H₂SO₄ solution reduces the anodic dissolution of mild steel and also retards the cathodic hydrogen evolution reaction. No definite trend was observed in the shift of E_{corr} values in the presence of various concentrations of these inhibitors in 0.5 M H₂SO₄ solutions. Inhibition efficiency $E_p(\%)$ increased with inhibitor concentrations for these inhibitors reaching a maximum value at concentration of (5×10^{-2} M) for all the studied inhibitors.

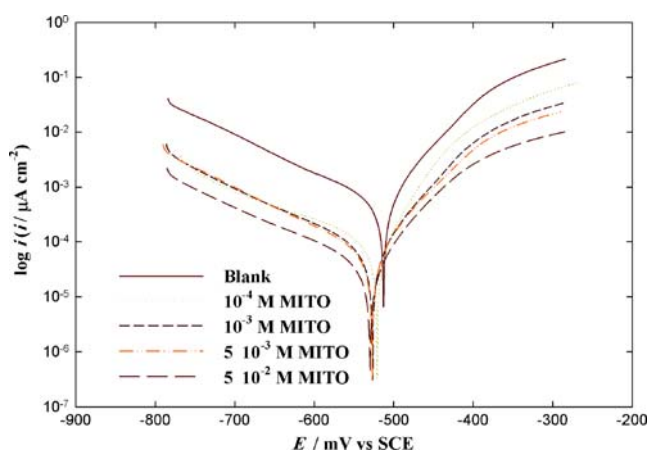


Fig. 6 Anodic and cathodic Tafel polarisation curves for mild steel in 0.5 M H₂SO₄ in the absence and presence of various concentrations of MITO at 25±1°C

It is well known that the spontaneous dissolution of steel in acids can be described by the anodic dissolution reaction



Accompanied by the corresponding cathodic reaction



The corrosion of steel in uninhibited acidic solutions is controlled by the hydrogen evolution reaction [65–67]. Following the electrochemical kinetic laws, the rates of the anodic and cathodic reactions in acidic solutions, in the presence of adsorbed inhibitor molecules on the metal surface, can be described by:

$$i_a = k_a(1 - \theta) \exp[Fz\beta(E - \psi_1)/RT] \quad (7)$$

$$i_c = k_c[\text{H}_3\text{O}^+](1 - \theta) \exp\{-F[\alpha E + (1 - \alpha)\psi_1]/RT\} \quad (8)$$

where k_a and k_c are the corresponding rate constants, θ is the fraction of the electrode surface covered by the inhibitor, E is the electrode potential relative to solution, ψ_1 is the potential drop in the outer part of the double layer, α and β are the symmetry factors of both reactions, while z is the charge of the metal ions in the solution.

It is assumed that hydrogen ionisation as well as the proceeding of electrochemical reactions can be neglected on the surface sites covered by the inhibitor molecules. Besides, it is accepted that the presence of Fe²⁺ (due to metal dissolution) on the uncovered surface has almost no effect. The studied methionine derivatives affect the rate of the corrosion process mainly through the variation of the

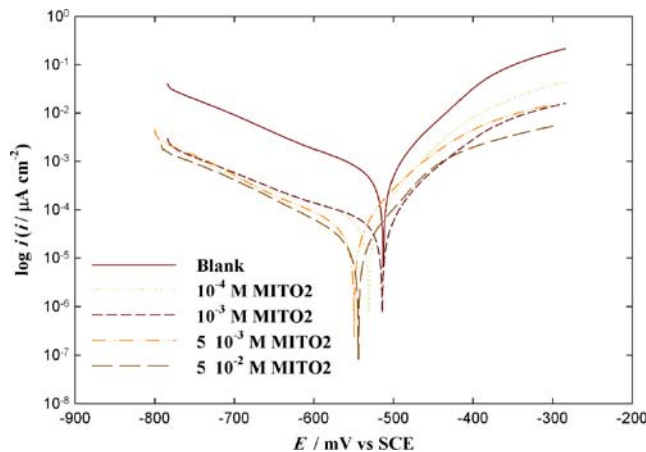


Fig. 7 Anodic and cathodic Tafel polarisation curves for mild steel in 0.5 M H₂SO₄ in the absence and presence of various concentrations of MITO2 at 25±1°C

Table 4 Electrochemical kinetic parameters obtained by Tafel polarisation technique for iron in absence and presence of various concentrations of methionine derivatives in 0.5 M H₂SO₄ at 25±1°C

	Conc. M	<i>i</i> _{corr} (μAcm ⁻²)	- <i>E</i> _{corr} (mV)	β _c (mV dec ⁻¹)	β _a (mV dec ⁻¹)	C.R mpy	<i>E</i> _p (%) (%)
MIT	Blank	798.1	512.8	186.0	85.59	364.8	
	10 ⁻⁴	215.5	517.7	185.7	98.52	98.49	72.99
	10 ⁻³	151.6	522.5	186.3	58.7	69.2	81.00
	5×10 ⁻³	111.73	517.9	190.5	81.22	51.05	86.00
	5×10 ⁻²	79.79	517.9	187.4	86.45	36.47	90.00
MITO	10 ⁻⁴	159.2	521.0	183.3	84.45	72.75	80.05
	10 ⁻³	104.2	526.4	181.8	87.1	47.61	86.94
	5×10 ⁻³	95.81	527	185.3	90.2	43.8	87.99
	5×10 ⁻²	63.90	529.8	189.9	100.5	29.21	91.99
	MITO2	10 ⁻⁴	103.7	531.4	193.0	86.0	47.42
10 ⁻³		86.17	514.3	187.1	91.72	39.39	89.20
5×10 ⁻³		63.91	549.6	176.3	95.12	29.21	91.99
5×10 ⁻²		40.0	544.1	182.6	105.0	18.29	94.98

degree of surface coverage, i.e. by blocking the effect they exert. The adsorption of the acid form of the inhibitor (cations) in outer Helmholtz plane (OHP) leads to a decrease of ψ₁, i.e. to its shift to more positive values. This in turn results in a decrease of the concentration of the hydrogen ions in the surface layer and a corresponding increase in the hydrogen evolution overpotential.

Electrochemical impedance spectroscopy

The key objective of EIS experiments is to provide an insight into the characteristics and kinetics of electrochemical processes occurring at the mild steel/H₂SO₄ interface in the absence and presence of methionine derivatives. The impedance response of these systems is presented in Figs. 8, 9 and 10. The Nyquist plots in Figs. 8, 9 and 10 generally have the

form of only one depressed semicircle, corresponding to one time constant in the Bode plots (not shown here). The results however clearly show a distinct concentration dependence of the effect of methionine derivatives on the corrosion inhibition efficiency.

The plots were similar for the three derivatives. Charge transfer resistance (*R*_t) is unequivocally correlated to the corrosion current density in relatively simple corrosion systems characterised by a charge transfer controlled process [68]. Semicircles are obtained, which cut the real axis at higher and lower frequencies. At higher frequency end, the intercept corresponds to *R*_s, and at lower frequency end, the intercept corresponds to *R*_s+*R*_t. The difference between these two values gives *R*_t. The results show that *R*_t values increased with increase of inhibitor concentration. The semicircle radii depend on the inhibitor concentration.

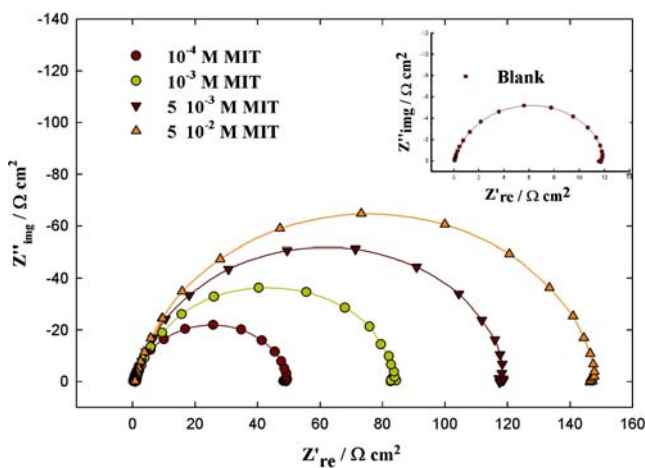


Fig. 8 Nyquist plots for iron in 0.5 M H₂SO₄ in the absence and presence of various concentrations of MIT at 25±1°C

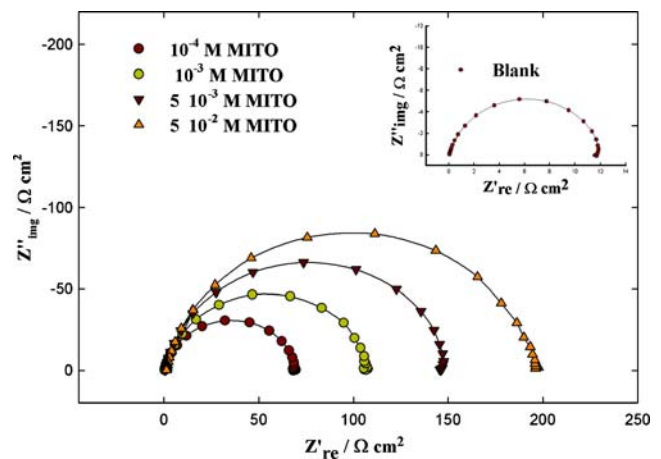


Fig. 9 Nyquist plots for iron in 0.5 M H₂SO₄ in the absence and presence of various concentrations of MITO at 25±1°C

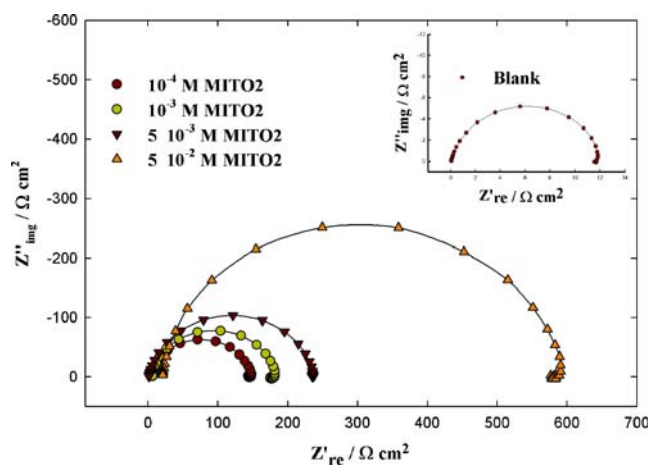


Fig. 10 Nyquist plots for iron in 0.5 M H₂SO₄ in the absence and presence of various concentrations of MITO2 at 25±1°C

The diameter of the capacitive loop increased with increase in methionine derivatives concentrations; the increase is significant in (MITO2). The Nyquist plots obtained in the real system represent a general behaviour where the double layer on the interface of metal/solution does not behave as a real capacitor. On the metal side, electrons control the charge distribution, whereas on the solution side, it is controlled by ions. As ions are much larger than the electrons, the equivalent ions to the charge on the metal will occupy quite a large volume on the solution side of the double layer [43].

The quantitative analysis of the electrochemical impedance spectra must be based on a physical model of the corrosion process with hydrogen depolarization and with charge transfer controlling step. The simplest model includes the electrochemical resistance in parallel to the double-layer capacitance connected with the resistance of the electrolyte. The solid electrode is inhomogeneous both on a microscopic and macroscopic scale, and corrosion is a uniform process with fluctuating active and inactive domains where anodic and cathodic reactions take place at the corroding surface. The size and distribution of these domains depend on the degree of surface inhomogeneities. Inhomogeneities may arise also from adsorption phenomena [62, 69, 70]. For this reason, the capacitance of the double layer at the metal/solution interface is modelled by the constant phase element (CPE). More generally, the CPE behaviour could be treated as a “ ω space fractality”, i.e. as manifestation of a self-similarity in the frequency domain [71]. The CPE impedance is given by Eq. 9, [69, 71–73]:

$$Z_{\text{CPE}} = \frac{1}{(i\omega)^n A} \quad (9)$$

where A is a proportionality coefficient and n has the meaning of the phase shift, the value of which can be

considered as a measure of the surface inhomogeneity [69, 70, 72, 74]. The transfer function is thus represented by an equivalent circuit, having only one time constant (Fig. 11). Parallel to the double-layer capacitance (simulated by a CPE) is the charge transfer resistance (R_t). The fitted parameter values are presented in Table 5. Table 5 shows that the presence of methionine derivatives increases the charge transfer resistance (R_t) values as the methionine derivatives concentrations increase, signifying a reduction in the corrosion rate. The corresponding percentage inhibition efficiencies $E_i(\%)$, respectively, increases from 77 to 98% as calculated from Eq. 10:

$$E_i(\%) = \left(1 - \frac{R_t^0}{R_t}\right) \times 100 \quad (10)$$

where R_t^0 and R_t represent the values of charge transfer resistance in absence and presence of methionine derivatives. The results also show that the presence of methionine derivatives at any concentration modified the interfacial capacitance, which suggests that these derivatives were adsorbed on the electrode surface at all concentrations. The decrease in C_{dl}/CPE values may be considered in terms of the Helmholtz model ($C_{dl} = \epsilon\epsilon_0 A/\delta$), where ϵ is the dielectric constant of the medium, ϵ_0 the vacuum permit-

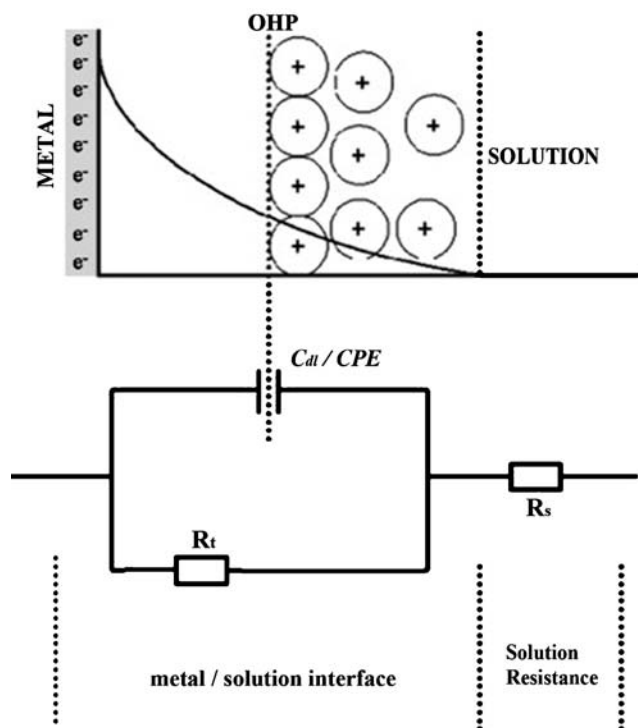


Fig. 11 Equivalent circuit used to model impedance data in 0.5 M H₂SO₄ solutions. OHP outer Helmholtz plane, CPE constant phase element, R_s solution resistance, R_t charge-transfer resistance

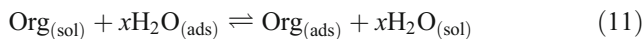
Table 5 Circuit element R_s , R_t , n , CPE values obtained using equivalent in Fig. 11 for iron in 0.5 M H_2SO_4 and different concentrations of methionine derivatives at $25 \pm 1^\circ C$

	Conc. M	R_s ($\Omega\text{ cm}^2$)	R_t ($\Omega\text{ cm}^2$)	CPE ($\mu F\text{cm}^{-2}$)	n	E_i (%)
	Blank	1.2	11.82	85.6	0.81	
MIT	10^{-4}	2.9	49.25	71.5	0.76	77.08
	10^{-3}	1.9	84.42	59.6	0.71	87.13
	5×10^{-3}	3.1	118.2	46.8	0.79	90.77
	5×10^{-2}	2.7	147.7	32.5	0.76	92.67
MITO	10^{-4}	2.6	69.529	68.6	0.78	84.13
	10^{-3}	2.8	107.45	38.5	0.76	89.85
	5×10^{-3}	2.2	147.75	26.7	0.83	92.70
	5×10^{-2}	2.5	197.00	16.2	0.84	94.53
MITO2	10^{-4}	2.6	147.75	52.2	0.78	92.68
	10^{-3}	2.8	181.84	36.5	0.71	94.06
	5×10^{-3}	2.4	236.4	26.2	0.85	95.46
	5×10^{-2}	2.6	591.0	13.4	0.81	98.19

tivity, A the electrode area and δ is the thickness of the protective layer. This is to suggest that the values of CPE/C_{dl} are always smaller in the presence of methionine derivatives than in their absence, as a result of effective adsorption of the inhibitors. Although the parameter n does not vary greatly, its value can be seen to decline at low methionine derivative concentrations due to increased surface roughness resulting from both methionine derivatives adsorption and enhanced corrosion rates.

Adsorption isotherm

It is generally accepted that organic molecules inhibit corrosion by adsorption at the metal/solution interface and that the adsorption depends on the molecule’s chemical composition, the temperature and the electrochemical potential at the metal/solution interface. In fact, the solvent H_2O molecules could also adsorb at metal/solution interface [75]. Therefore, the adsorption of organic inhibitor molecules from the aqueous solution can be regarded as a quasi-substitution process between the organic compound in the aqueous phase $[Org_{(sol)}]$ and water molecules at the electrode surface $[H_2O_{(ads)}]$ [76].



where x is the size ratio, that is, the number of water molecules replaced by one organic inhibitor. Basic information on the adsorption of inhibitor on metals surface can be provided by adsorption isotherm. Attempts were made to fit experimental data to various isotherms including Frumkin, Langmuir, Temkin, Freundlich, Bockris–Swinkels and Flory–Huggins isotherms. All these isotherms are of the general form [76]

$$f(\theta, x) \exp(-2\alpha\theta) = Kc \tag{12}$$

where $f(\theta, x)$ is the configurational factor, which depends upon the physical mode and the assumptions underlying the derivation of the isotherm, θ is the degree of surface coverage, c is the concentration of the adsorbate in the bulk solution, x is the size ratio factor, α is the molecular interaction parameter and K is the equilibrium constant of the adsorption process. In this study, the results were best fitted by Temkin adsorption isotherm, Eq. 13 [77].

$$\log(\theta/C) = \log K - g\theta \tag{13}$$

The Temkin isotherm presented in Fig. 12, showed a good correlation with experimental data. The negative slope g indicates the existence of a repulsive lateral interaction in the adsorption layer. The free-energy of adsorption (ΔG_{ads}) was calculated from the intercept of Temkin isotherm,

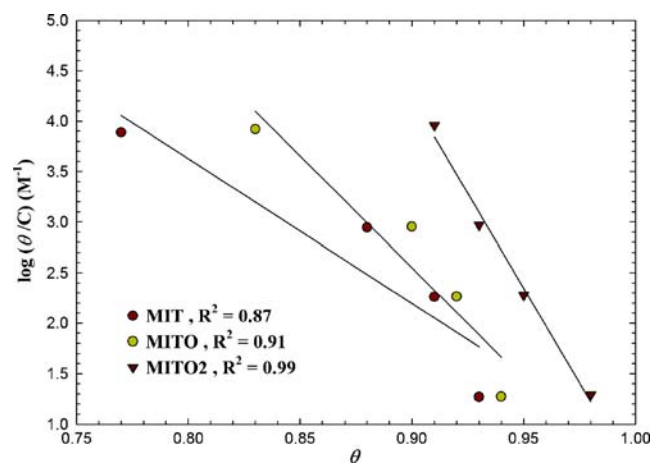


Fig. 12 Temkin adsorption plots of iron in 0.5 M H_2SO_4 containing various concentrations of methionine derivatives at $25 \pm 1^\circ C$

which showed correlation with the experimental data, according to Eq. 14:

$$K = \frac{1}{55.5} \exp(-\Delta G_{\text{ads}}^{\circ}/RT) \quad (14)$$

where 55.5 is the water concentration, R the universal gas constant and T the thermodynamic temperature. The adsorption–desorption equilibrium constant K was determined from the intercept and by compensation in Eq. 14, leading to $\Delta G_{\text{ads}}^{\circ} = -94.32$, -135.72 and -222.55 kJ mol⁻¹ for MIT, MITO and MITO2, respectively. The negative values of $\Delta G_{\text{ads}}^{\circ}$ means that the adsorption process is spontaneous, while the high values of $\Delta G_{\text{ads}}^{\circ}$ indicate that methionine derivatives were chemically adsorbed on the mild steel surface.

The validity of Temkin's isotherm favours the assumption of a chemisorptive bond between the steel surface and the methionine molecules [78], i.e. the unshared electron pairs in N, O and S atoms of methionine derivatives could interact with d-orbitals of iron to provide a protective chemisorbed film.

The free adsorption energies calculated from Temkin adsorption isotherm are in line with adsorption energies calculated from Monte Carlo simulation method. The difference in the values of adsorption energy calculated from Monte Carlo simulations and Temkin adsorption isotherm could be explained by adsorption of surface aggregates. Although it appears that the adsorbate structure on corroding metals has not been investigated, it is quite possible that such structures form in the initial stage of adsorption [79].

Inhibition mechanism

The increase in efficiency of inhibition of methionine derivatives determined by various chemical and electrochemical techniques, with their concentrations, indicates that these derivatives are adsorbed on the mild steel surface at higher concentration, leading to greater surface coverage (θ). It is generally accepted that the first step in the adsorption of an organic inhibitor on a metal surface usually involves the replacement of one or more of water molecules adsorbed at the metal surface [80].

The mixed-inhibition mechanism suggested by the polarisation data is consistent with the findings of Oguzie et al. [81] and those of El Azhar et al. [68] on the adsorption behaviour of organic molecules containing both N and S atoms. In acid solutions, organic inhibitors may interact with the corroding metal and hence affect the corrosion reaction in more than one way, sometimes simultaneously. It is therefore often difficult to assign a single general inhibition mechanism, since the mechanism

may change with experimental conditions. S-containing compounds have been shown to preferentially chemisorb on the surface of mild steel in acidic media, whereas N-containing substances tend to favour physisorption [82]. Again, the presence of more than one functional group has been reported to often lead to changes in the electron density of a molecule, which could influence its adsorption behaviour [83].

In this study, methionine derivatives are studied computationally in its neutral form. Methionine derivatives can also present as protonated species in sulphuric acid solutions. Both molecular and protonated species can adsorb on the metal surface. The adsorption of methionine derivatives through the ammonium group ($-\text{NH}_4^+$) can occur on the pre-adsorbed sulphate anions even though the presence of S-CH₃ group decreases the stability of the positive charge. Adsorption of the protonated methionine derivatives on the cathodic sites on mild steel surface retards the hydrogen evolution reaction. Adsorption on the anodic sites of mild steel surface occurs via S atom in the aliphatic chain in case of MIT, S=O group in case of MITO or SO₂ group in case of MITO2 to retard mild steel dissolution process. Adsorption of methionine derivatives on mild steel surface are assisted by hydrogen bond formation (Fig. 3 and Table 1) between methionine derivatives and the steel surface. This type of adsorption should be more prevalent for protonated inhibitors, because the positive charge on the N-atom is conducive to the formation of hydrogen bonds. Unprotonated N-atoms may adsorb by direct chemisorption or by hydrogen bonding [84]. Methionine derivatives thus have the ability to influence both the cathodic and anodic partial reactions, giving rise to the mixed inhibition mechanism observed.

Conclusions

With contrast to the traditional technique of identifying new corrosion inhibitors in wet-lab, a prior dry-lab process, followed by wet-lab process is suggested by using cheminformatics tools. The following results can be concluded from this study:

- Monte Carlo simulations technique incorporating molecular mechanics and molecular dynamics can be used to simulate the adsorption of methionine derivatives on iron (110) surface in 0.5 M sulphuric acid.
- The quantum mechanical approach may well be able to foretell molecule structures that are better for corrosion inhibition.
- Methionine derivatives have a very good inhibitive effect for corrosion of mild steel in 0.5 M sulphuric acid solution.

- Potentiodynamic polarisation studies have shown that methionine derivatives act as mixed-type inhibitors, and their inhibition mechanism is adsorption-assisted by hydrogen bond formation.
- Impedance results indicate that the values of CPEs tend to decrease with increasing inhibitor concentrations due to the increase of the thickness of the electrical double layer. Both polarisation resistance and inhibition efficiency $E_i(\%)$ tend to increase with increasing inhibitor concentrations due to the increase of the surface coverage of the inhibitors, i.e. the decrease of the electrochemical active surface area.

References

1. Oguzie EE (2006) Mater Chem Phys 99:441. doi:10.1016/j.matchemphys.2005.11.018
2. Oguzie EE (2005) Pigment Resin Technol 34:321. doi:10.1108/03699420510630336
3. Oguzie EE, Iyeh KL, Onuchukwu AI (2006) Bull Electrochem 22:63
4. Zhao YL, Liang PQ, Hou B (2005) Appl Surf Sci 252:1245. doi:10.1016/j.apsusc.2005.02.094
5. Morad MS, El-Hagag A, Hermas A, Abdel Aal MS (2002) J Chem Technol Biotechnol 77:486. doi:10.1002/jctb.588
6. Moretti G, Guidi F, Grion G (2004) Corros Sci 46:387. doi:10.1016/S0010-938X(03)00150-1
7. Oliveres O, Likhanova NV, Gomez B, Navarrete J, Llanos-Serrano ME, Arce E, Hallen JM (2006) Appl Surf Sci 252:2894. doi:10.1016/j.apsusc.2005.04.040
8. Zhang DQ, Gao LX, Zhou GD (2003) J Appl Electrochem 33:361. doi:10.1023/A:1024403314993
9. Oguzie EE, Unaegbu C, Ogukwe CN, Okolue BN, Onuchukwu AI (2004) Mater Chem Phys 84:363. doi:10.1016/j.matchemphys.2003.11.027
10. Shibli SMA, Saji VS (2005) Corros Sci 47:2213. doi:10.1016/j.corsci.2004.09.012
11. Mu G, Li X (2005) J Colloid Interface Sci 289:184. doi:10.1016/j.jcis.2005.03.061
12. Feng Y, Siow KS, Teo WK, Hsieh AK (1999) Corros Sci 41:829. doi:10.1016/S0010-938X(98)00144-9
13. Aksut AA, Bilgic S (1992) Corros Sci 33:379. doi:10.1016/0010-938X(92)90067-D
14. Bilgic S, Aksut AA (1993) Br Corros J 28:59
15. Abdel-Aal MS, Morad MS, Ahmed ZA (1995) Ann Univ Ferrara Sez 10:343
16. Trabaneli G (1987) Corrosion inhibitors. In: Mansfeld F (ed) Chemical industries: corrosion mechanism. Marcel Dekker, New York
17. Schmitt G (1984) Br Corros J 19:165
18. Morad MS (2005) J Appl Electrochem 35:889. doi:10.1007/s10800-005-4745-2
19. Abd-El-Nabey BA, Khalil N, Mohamed A (1985) Surf Technol 24:383. doi:10.1016/0376-4583(85)90056-1
20. Abiola OK (2005) J Chil Chem Soc 50:685
21. Abiola OK, Oforka NN, Ebenso EE (2004) Bull Electrochem 20:409
22. Oguzie EE, Li Y, Wang FH (2007) J Colloid Interface Sci 310:90. doi:10.1016/j.jcis.2007.01.038
23. Oguzie EE, Li Y, Wang FH (2007) Electrochim Acta 52:6988. doi:10.1016/j.electacta.2007.05.023
24. Ashassi-Sorkhabi H, Ghasemi Z, Seifzadeh D (2005) Appl Surf Sci 249:408. doi:10.1016/j.apsusc.2004.12.016
25. Li SL, Wang YG, Chen SH (1999) Corros Sci 41:1769. doi:10.1016/S0010-938X(99)00014-1
26. Bereket G, Hur E, Ogretir C (2002) J Mol Struct 578:79
27. Khalil N (2003) Electrochim Acta 48:2635. doi:10.1016/S0013-4686(03)00307-4
28. Rodriguez-Valdez LM, Martinez-Villafane A, Glossman-Mitnik D (2005) J Mol Struct 713:65
29. Tang ZL, Song SZ (1995) J Chin Soc Corros Prot 15:229
30. Vosta J, Eliásek J (1971) Corros Sci 11:223. doi:10.1016/S0010-938X(71)80137-3
31. Costa JM, Lluich JM (1984) Corros Sci 24:929. doi:10.1016/0010-938X(84)90113-6
32. Zhang JC, Cao WL, Wang ZX (1986) J Chin Soc Corros Prot 6:217
33. Abdul-Ahad PG, Al-Madfaei SF (1989) Corrosion 45:978
34. Wang DX, Xiao HM (2000) J Mol Sci 16:102
35. Kantarci N, Tamerler C, Sarikaya M et al (2005) Polymer 46:4307
36. Swiler TP, Loehman RE (2000) Acta Mater 48:4419. doi:10.1016/S1359-6454(00)00228-7
37. Lindenblatt M, van Heys J, Pehlke E (2006) Surf Sci 600:3624. doi:10.1016/j.susc.2006.01.066
38. Kornherr A, French SA, Sokol AA (2004) Chem Phys Lett 393:107. doi:10.1016/j.cplett.2004.06.019
39. Kornherr A, Hansal S, Hansal WEG (2003) J Chem Phys 119:9719. doi:10.1063/1.1615491
40. Mutombo P, Hackerman N (1998) Anti-Corros Methods Mater 45:413. doi:10.1108/00035599810236559
41. Martinez S (2003) Mater Chem Phys 77:97. doi:10.1016/S0254-0584(01)00569-7
42. Bouklah M, Benchat N, Aouniti A, Hammouti B, Benkaddour M, Lagrenée M, Vezin H, Bentiss F (2004) Prog Org Coat 51:118. doi:10.1016/j.porgcoat.2004.06.005
43. Özcan M, Dehri İ, Erbil M (2004) Appl Surf Sci 236:155. doi:10.1016/j.apsusc.2004.04.017
44. Babić-Samardžija K, Hackerman N (2005) J Solid State Electrochem 9:483. doi:10.1007/s10008-004-0584-z
45. Ashassi-Sorkhabi H, Shaabani B, Seifzadeh D (2005) Electrochim Acta 50:3446. doi:10.1016/j.electacta.2004.12.019
46. Cruz J, Pandiyan T, García-Ochoa E (2005) J Electroanal Chem 583:8. doi:10.1016/j.jelechem.2005.02.026
47. Benali O, Larabi L, Mekelleche SM, Yarek Y (2006) J Mater Sci 41:7064. doi:10.1007/s10853-006-0942-6
48. Gómez B, Likhanova NV, Domínguez-Aguilar MA, Martínez-Palou R, Vela A, Gazquez JL (2006) J Phys Chem B 110:8928. doi:10.1021/jp057143y
49. Bentiss F, Gassama F, Barbry D, Gengembre L, Vezin H, Lagrenée M, Traisnel M (2006) Appl Surf Sci 252:2684. doi:10.1016/j.apsusc.2005.03.231
50. Rodriguez-Valdez LM, Casales M, González-Rodríguez JG, Martínez-Villafañe A, Martínez L, Glossman-Mitnik D (2006) Corros Sci 48:4053. doi:10.1016/j.corsci.2006.05.036
51. Gao G, Liang C (2007) Electrochim Acta 52:4554. doi:10.1016/j.electacta.2006.12.058
52. Li W, He Q, Pei C, Hou B (2007) Electrochim Acta 52:6386. doi:10.1016/j.electacta.2007.04.077
53. Bentiss F, Lebrini M, Lagrenée M, Traisnel M, Elfarouk A, Vezin H (2007) Electrochim Acta 52:6865. doi:10.1016/j.electacta.2007.04.111
54. Popova A, Christov M, Zwetanova A (2007) Corros Sci 49:2131. doi:10.1016/j.corsci.2006.10.021
55. Lebrini M, Lagrenée M, Vezin H, Traisnel M, Bentiss F (2007) Corros Sci 49:2254. doi:10.1016/j.corsci.2006.10.029
56. Barriga J, Coto B, Fernandez B (2007) Tribol Int 40:960. doi:10.1016/j.triboint.2006.02.030

57. Sun H, Ren P, Fried JR (1998) *Comput Theor Polymer Sci* 8:229. doi:10.1016/S1089-3156(98)00042-7
58. Metropolis N, Rosenbluth AW, Rosenbluth MN, Teller AH, Teller EJ (1953) *J Chem Phys* 21:1087. doi:10.1063/1.1699114
59. Roothaan CCJ (1951) *Rev Mod Phys* 23:69. doi:10.1103/RevModPhys.23.69
60. HyperChem (2002) Hypercube Inc, Gainesville
61. Leunberger DG (1973) *Intruduction to linear and non-linear programming*. Addison-Wesley, Don Mills
62. Juttner K (1990) *Electrochim Acta* 35:1501. doi:10.1016/0013-4686(90)80004-8
63. Wang CT, Chen SH, Ma HY, Qi CS (2003) *J Appl Electrochem* 33:179. doi:10.1023/A:1024097208128
64. Fang Y, Li J (2002) *J Mol Struct Theochem* 593:179. doi:10.1016/S0166-1280(02)00316-0
65. Zhuk NP (1976) *Course in corrosion and metal protection*. Metallurgy, Moscow
66. Antropov AI, Makushin EM, Panasenko VP (1981) *Inhibitors of metal corrosion*. Tekhnika, Kiev
67. Reshetnikov SM (1986) *Inhibitors of metal acid corrosion*. Khimiya, Leningrad
68. MEI A, Memari B, Traisnel M, Bentiss F, Lagrenee M (2001) *Corros Sci* 43:2229. doi:10.1016/S0010-938X(01)00034-8
69. Growcock FB, Jasinski RJ (1989) *J Electrochem Soc* 136:2310. doi:10.1149/1.2097847
70. Rammelt U, Reinhard G (1987) *Corros Sci* 27:373. doi:10.1016/0010-938X(87)90079-5
71. Stoynov Z (1990) *Electrochim Acta* 35:1493. doi:10.1016/0013-4686(90)80003-7
72. Stoynov ZB, Grafov BM, Savova-Stoynova B, Elkin VV (1991) *Electrochemical impedance*. Nauka, Moscow
73. Macdonald JR (1987) *J Electroanal Chem* 223:25. doi:10.1016/0022-0728(87)85249-X
74. Lopez DA, Simison SN, Sanchez SR (2003) *Electrochim Acta* 48:845. doi:10.1016/S0013-4686(02)00776-4
75. Li X, Deng S, Fu H, Mu G (2009) *Corros Sci* 51:620. doi:10.1016/j.corsci.2008.12.021
76. Sahin M, Bilgic S, Yilmaz H (2002) *Appl Surf Sci* 195:1. doi:10.1016/S0169-4332(01)00783-8
77. Cardoso SP, Reis FA, Massapust FC, Costa JF, Tebaldi LS, Araújo LFL, Silva MVA, Oliveira TS, Gomes JACP, Hollauer E (2005) *Quim Nova* 28:756
78. Stoyanova AE, Sokolova EI, Baicheva SN (1997) *Corros Sci* 39:1595. doi:10.1016/S0010-938X(97)00063-2
79. Knag M, Sjöblom J, Øye G, Gulbrandsen E (2005) *Colloids Surf A Psychochem Eng Asp* 250:269
80. Bockris JO, Swinkels DAJ (1964) *J Electrochem Soc* 11:736. doi:10.1149/1.2426222
81. Oguzie EE, Onuoha GN, Onuchukwu AI (2004) *Mater Chem Phys* 89:305. doi:10.1016/j.matchemphys.2004.09.004
82. Fragnani A, Trabanelli G (1999) *Corrosion* 55:653
83. Hackerman N, Cook EL (1950) *J Electrochem Soc* 97:2
84. Khaled KF, Amin MA (2008) *J Appl Electrochem* 38:609. doi:10.1007/s10800-008-9604-5